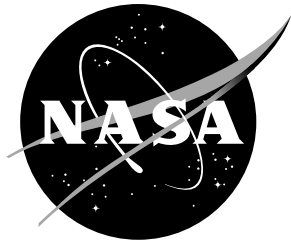


NASA Technical Memorandum 110311



Research and Applications in Structures at the NASA Langley Research Center

Irving Abel
Langley Research Center, Hampton, Virginia

January 1997

National Aeronautics and
Space Administration
Langley Research Center
Hampton, Virginia 23681-0001

RESEARCH AND APPLICATIONS IN STRUCTURES AT THE NASA LANGLEY RESEARCH CENTER

Irving Abel
NASA Langley Research Center
Hampton, Virginia USA

ABSTRACT

An overview of recently completed programs in structures research at the NASA Langley Research Center is presented. Also included is a description of the unique facilities used to support the structures program. Methods used to perform flutter clearance studies in the wind-tunnel on a high performance fighter are discussed. Recent advances in the use of smart structures and controls to solve the aeroelastic problems of fixed- and rotary-wing vehicles, including flutter, loads, vibrations, and structural response are presented. The use of photogrammetric methods in space to measure spacecraft dynamic response is discussed. The use of advanced analytical methods to speed up detailed structural analysis is presented. Finally, the application of cost-effective composite materials to wing and fuselage primary structures is illustrated.

INTRODUCTION

The Langley Research Center (LaRC) has been designated the NASA "Center of Excellence" for Structures and Materials research. The Structures Division at LaRC conducts analytical and experimental research (figure 1) in Aeroelasticity, Structural Mechanics, Computational Structures, Structural Dynamics, and Thermal Structures to meet the technology requirements for advanced aerospace vehicles. The charter for each research area is given in figure 2.

The Structures Division supports the development of more efficient structures for airplanes, helicopters, spacecraft, and space transportation vehicles. Analytical methods for improving structural analysis and design are developed and validated by experimental methods. New structural concepts for both metal and composite structures are developed and evaluated through laboratory testing. Research is conducted to integrate advanced structural concepts with active-control concepts and smart materials to enhance structural performance. Studies of impact dynamics focus on

increased survivability in the case of crash impact. Research in thermal structures is aimed at efficient structural concepts for future high-speed aircraft and space transportation systems that exploit the benefits of advanced composite and metallic materials. Research in aeroelasticity ranges from flutter clearance studies of new vehicles using aeroelastic models tested in the wind tunnel, to the development of new concepts to control aeroelastic response, and to the acquisition of unsteady pressures on wind-tunnel models for providing experimental data to validate unsteady theories. Analytical methods are developed and validated to solve the aeroelastic problems of fixed- and rotary-wing vehicles, including the control of instabilities, loads, vibration, and adverse structural response.

This paper presents a brief overview of the test facilities operated by the Structures Division and the results of some selected studies in structural mechanics and dynamics during the last 2 years. This paper begins with an overview of how flutter clearance studies are performed in the wind tunnel. The paper then addresses research aimed at using smart materials to suppress aeroelastic response, at acquiring an experimental data base to validate computational fluid dynamics codes, at the use of smart materials and control surfaces to reduce the buffeting response of a modern twin-tail fighter, at the use of flaperons to control tiltrotor vibratory loads, at using advanced photogrammetric methods to measure the dynamic response of spacecraft in orbit, at developing new computational methods that significantly reduces the time and cost to perform structural analysis, at the use of advanced concepts to improve the survivability of occupants in a composite aircraft during a crash, and at a program to exploit the use of composites in primary structure of advanced transport aircraft.

EXPERIMENTAL FACILITIES

The structures research program at LaRC requires the support of a unique set of experimental facilities. These facilities include the Transonic Dynamics Tunnel, the Structural Mechanics

Laboratory, the Aircraft Landing Dynamics Facility, the Impact Dynamics Research Facility, the Thermal Structures Laboratory, the Structural Dynamics Laboratory, and the Combined Loads Testing System (figure 3). Replacement value of these facilities is estimated to be in excess of \$350 million U.S. dollars.

A short description of each of these experimental facilities follows:

Transonic Dynamics Tunnel

The Transonic Dynamics Tunnel (TDT) is a unique "national" facility dedicated to identifying, understanding, and solving aeroelastic problems. The TDT is a closed-circuit, continuous-flow, variable-pressure, wind tunnel with a 16-foot square test section. The tunnel uses either air or a heavy gas as the test medium and can operate at stagnation pressures from near vacuum to atmospheric, has a Mach number range from near zero to 1.2, and is capable of maximum Reynolds numbers of about 3 million per foot in air to 10 million per foot in heavy gas. The TDT is specially configured for flutter testing, with excellent model visibility from the control room and a rapid tunnel shutdown capability for model safety. Model mount systems include two sidewall turntables for semispan models, a variety of stings for full-span models, a cable-mount system for "flying" models, a rotorcraft testbed for rotor blade loads research, and a floor turntable for launch vehicle ground-wind loads studies. The TDT also offers an airstream oscillation system for gust studies and supporting systems for active controls testing. Testing in heavy gas has important advantages over testing in air including improved model to full-scale similitude, higher Reynolds numbers, and reduced tunnel power requirements. The TDT is the only wind tunnel in the world capable of flutter testing large, full-span, aeroelastically-scaled models at transonic speeds.

Structural Mechanics Laboratory

Built in 1939 to contribute to the development and validation of aircraft structural designs during World War II, this laboratory currently supports a broad range of structural and materials development activities for advanced aerospace structures. Static testing, environmental testing, and material fabrication and analysis are performed. Emphasis is

on the development of structural mechanics technology and advanced structural concepts enabling the verified design of efficient, cost-effective, damage-tolerant, advanced-composite structural components subjected to complex loading and demanding environmental conditions. This facility contains unique specially designed 120-, 300-, and 1,200-kip test machines with special platens for precision compression testing and a strong-back load-reaction structure capable of testing large test specimens subjected to loads from multiple hydraulic actuators.

Aircraft Landing Dynamics Facility

The Aircraft Landing Dynamics Facility (ALDF) is a test track used primarily for landing gear, tire, and runway surface research studies. The ALDF uses a high-pressure water-jet system to propel a test carriage down a 2800-ft track. The propulsion system consists of a vessel that holds 28000 gallons of water pressurized up to 3150 psi. A quick-opening shutter valve releases a high energy water jet, which catapults the carriage to the desired speed. The propulsion system produces a thrust in excess of 2 million lbs, which is capable of accelerating the 54-ton test carriage to speeds of 220 knots within 400 ft. This thrust creates a peak acceleration of approximately 20g's on the carriage. The carriage coasts through an 1800-ft test section and decelerates to a velocity of 175 knots or less before it intercepts five arresting cables that span the track at the end of the test section. The arresting system brings the test carriage to a stop in 600 ft or less. Essentially, any aircraft landing gear and tire can be mounted on the test carriage and virtually any runway surface and weather condition can be duplicated on the track.

Impact Dynamics Research Facility

The Langley Impact Dynamics Research Facility is used to conduct crash testing of small full-scale aircraft under controlled conditions. Using a pendulum method, aircraft (maximum weight 30,000 lbs) are suspended by cables from the 240 feet high gantry and swung into impact surfaces--either soil or concrete. Free flight conditions are established when the swing cables are pyrotechnically separated from the vehicle just prior to impact. Flight path angles at impact may be varied from 0° to -60°. The maximum velocity obtainable, without rocket assistance, is approximately 88 ft/sec (60 mph). Instrumentation for these tests include

on-board cameras, strain gages, load cells, displacement transducers, and accelerometers. Transducers in the aircraft are hard-wired through a long umbilical cable to the data acquisition room.

Thermal-Structures Laboratory

The Thermal-Structures Laboratory is used to conduct a broad range of research to characterize the behavior of advanced thermal-structures subjected to combined thermal and mechanical loading conditions. The structures can be passively and/or actively cooled and range from innovative lightweight, durable thermal protection systems and cryogenic propellant tanks for reusable launch vehicles to actively cooled engine and stagnation region structures for hypersonic air breathing vehicles. This facility contains one 22 kip, one 110 kip, three 220 kip, and two 500 kip servo-hydraulic load machines. Thermal/mechanical load tests can be conducted under the application of high thermal loads with a temperature range of -420°F to 2500°F on specimens that are up to 4 ft by 8 ft in size.

Structural Dynamics Laboratory

The Structural Dynamics Laboratory consists of two facilities designed for structural dynamics and pointing control research on aerospace structures and components: 1.-The Dynamics Test and Research Laboratory (DTRL) is a 5,200 square ft, 80-ft-high building equipped with advanced suspension devices. The photograph in figure 3 shows a model of a spacecraft under dynamics testing in the DTRL. This facility has a large data acquisition system for acquiring dynamic data. 2.-The Structural Dynamics Research Laboratory (SDRL) has a 38-ft-high vertical backstop and a 12- by 12- by 95-ft tower. These facilities are supported by dynamic test and signal processing equipment including 10-in.-stroke shakers, near-zero spring-rate suspension systems, an arc-second attitude measurement system, data acquisition, a real-time control computer, video monitoring, and environmental controls.

Combined Loads Testing System - COLTS

The Combined Loads Test System (COLTS) is being developed at the Langley Research Center and will be a unique structures research test facility. This facility will enable complex, combined loads testing of large aerospace structures under

representative operating conditions. Typical aerospace structures will include panels from transport aircraft fuselages, full fuselage barrels, and panels from launch vehicles. The COLTS will consist of two Pressure Box Test Machines and a Combined Loads Test Machine. One Pressure Box Test Machine is currently operational (Figure 4a) and is used to apply pneumatic pressure (up to 20 psig) to curved panel specimens to achieve a biaxial tension stress field at ambient conditions. Load actuators apply additional longitudinal loads of up to 450 kips to the specimen. Typical test specimens are 72 in. long and 63 in. wide, and have a radius of 125 in. A second Pressure Box Test Machine will be used to conduct biaxial tension testing at elevated and cryogenic conditions.

The Combined Loads Test Machine is under construction (anticipated startup date November 1997). This test machine will be able to apply combined mechanical, pneumatic pressure, and thermal loadings to broad classes of aerospace structures including panel and barrel specimens (Figure 4b). The Combined Loads Test Machine will have a 2700-kip axial load, a 600-kip vertical shear load, a 6000-ft-kip torsion load, and a 20-psig pressure load capacity. Specimens may be tested at temperatures up to 400°F, and at cyclic, spectrum fatigue loading conditions. Typical test specimens would include curved panels that are 120 in. long and 96 in. wide, and have a radius of 125 in. as well as full shells that are as much as 45 ft long and 15 ft in diameter.

This paper will now present selected results of some recent studies in the areas of structural dynamics and mechanics.

F/A-18E/F FLUTTER CLEARANCE

The Transonic Dynamics Tunnel plays a significant role in providing flutter clearance data for new aircraft configurations. Tunnel tests performed on an aeroelastic model tested in a heavy gas can be used to predict the aeroelastic characteristics of the full-scale vehicle flying in the atmosphere. This information can then be used to minimize the flutter risk of new configurations, to provide data so that full-scale calculations can be performed with greater confidence, and to minimize the time required to perform airplane flutter clearance flights. When military fighters are tested in the tunnel many different store configurations can be cleared with relative speed and safety.

Such an example is the F-18E/F flutter studies recently completed in the TDT. The flutter clearance study utilized a full-span 18-percent scale model. As shown in figure 5, the model can be sting- or cable-mounted in the test section. Before flutter testing commenced, a rigid model was tested on the cable-mount system to assure flying stability in the tunnel. During tests in the TDT the following accomplishments were achieved; the flexible vehicle components were flutter cleared through $M=1.2$ on the sting mount, the flexible wing and fuselage configuration were cleared for flutter on the cable-mount system, numerous store configurations were flutter cleared on the cable-mount system, the stability of all-moveable stabilators with mil-spec freeplay was verified, and the stability of the model with several failure modes was determined. Limited parametric studies were also performed to determine the effect of stabilator free play, wing and fuselage fuel, wing-tip-and wing-pylon-mounted stores/tanks, and control surface restraint springs on flutter.

PIEZOELECTRIC AEROELASTIC RESPONSE TAILORING INVESTIGATION

The Piezoelectric Aeroelastic Response Tailoring Investigation (PARTI) was the first study in which piezoelectric materials were chosen to control the aeroelastic response of a relatively large, aeroelastic model. Piezoelectric materials possess the ability to develop a mechanical strain when subjected to an electrical charge. Therefore, piezoelectric materials can be used as actuators to control aeroelastic motion. The relationship between an applied electric field and the corresponding behavior of a piezoelectric actuator is well documented in [1, 2, 3]. The conventional configuration for an in-plane displacement piezoelectric actuator consists of a single piezoelectric wafer sandwiched between two electrodes. Increased in-plane actuation can be obtained by grouping multiple wafers into multiple layers.

The model, shown in figure 6a, is a five-foot long, high-aspect-ratio semi-span wing designed to flutter in the TDT. The model is comprised of an exterior fiberglass shell to provide the proper aerodynamic contour and an interior composite plate as the main load carrying structure. A sketch of the major components of the PARTI wing are shown in figure 6b. Piezoelectric actuator patches were attached to the upper and lower surfaces of the composite plate. Fifteen groups of piezoelectric actuator

patches covered the inboard 60% of the span. Due to the ply orientation of the material used in the composite plate and the wing sweep, the actuators were able to affect both the bending and torsional response of the model. Ten strain gauges and four accelerometers were used as sensors to provide feedback signals to the piezoelectric actuators. The model is also equipped with wing-tip flutter-stopper and a trailing-edge control surface. The flutter-stopper was used as a safety device during wind-tunnel testing.

The purpose of the study was to demonstrate an increase in flutter dynamic pressure and a reduction in subcritical response by using piezoelectric actuators. Experimental open-loop flutter characteristics and response time histories below the flutter boundary as a function of each piezoelectric actuator group were first determined in the TDT. These results were then used to design control laws to suppress flutter and reduce the aeroelastic response. Twenty-eight control laws were designed and tested. Control laws were designed using both single-input/single-output (SISO) and multi-input/multi-output (MIMO) methods that utilized up to five inputs and nine outputs. Each control law varied in design technique, actuator and sensor choices, and complexity of the controller. The most successful control law demonstrated a 12% increase in flutter dynamic pressure and reduced the power spectral density of peak response due to tunnel turbulence at subcritical speeds by 75%. These experimental results are shown in figure 7.

The PARTI program successfully demonstrated the control of aeroelastic response using piezoelectric actuators on a large aeroelastic model tested in the TDT. Results of this investigation are fully documented in [4, 5, 6].

BENCHMARK ACTIVE CONTROLS TECHNOLOGY

The Benchmark Active Controls Technology (BACT) model is one of a series of five wind-tunnel models developed for the Benchmark Models Program (BMP). The original goal of the BMP was to obtain experimental data for validating unsteady CFD codes. An example of the type of data acquired in this program is presented in [7]. The BMP uses highly instrumented rigid models that are tested in the TDT on a flexible sidewall mount known as the Pitch and Plunge Apparatus or

“PAPA”. It provides the two degrees of freedom that are required for classical flutter [8]. Unsteady pressure distributions can then be obtained during sustained model oscillations at flutter onset and can be compared with analytical predictions.

The objectives of the current BACT model tests are to: obtain high quality data to validate computational-fluid-dynamics and computational-aeroelasticity codes; to verify the accuracy of current aeroservoelastic design and analysis tools; and to provide an active controls testbed for evaluating new and innovative control methodologies. Some early results for this BACT model are presented in [9]. The model has a rectangular planform with an NACA 0012 airfoil section and is equipped with a trailing-edge control surface and a pair of independently actuated upper and lower-surface spoilers. All surfaces are moved with independent miniature hydraulic actuators. A photograph of the model on the “PAPA” mount system is shown in figure 8a and a view of the model mounted in the wind tunnel is shown in figure 8b. Instrumentation includes pressure transducers and accelerometers on the model, and strain gages on the mount-system.

During a recent BACT wind-tunnel test entry the primary objective was to investigate a variety of control algorithms, designed using various methods, to suppress flutter and alleviate gust loads. The plot in figure 9a presents the performance of three semi-adaptive flutter-suppression control laws. The solid line is the open-loop flutter boundary of the BACT model. The circle symbols correspond to the points where control laws were tested. The GPC control law used a Generalized Predictive Control algorithm and employed an analytical representation of the plant to predict future model responses and select control surface commands to minimize that response. The Inverse Control used linear neural networks to learn the plant inverse and employed experimental data. The NPC system used a Neural Predictive Control (NPC) algorithm. All control laws used only the trailing-edge control surface. As indicated in the figure, all three semi-adaptive systems were very successful in suppressing flutter. Figure 9b presents open- and closed-loop model responses due to flow oscillations produced by the TDT flow oscillator system. Oscillation frequencies ranged from zero to 5.5 Hz. The NPC control law was a gust load alleviation

design and reduced acceleration responses by up to 80%.

ACTIVELY CONTROLLED RESPONSE OF BUFFET AFFECTED TAILS

Buffeting is an aeroelastic phenomenon which plagues high performance aircraft, especially those with twin-vertical-tails. For aircraft of this type at high angles of attack, vortices emanating from wing/fuselage leading-edge extensions burst, immersing the vertical tails in their wake. As shown in figure 10, for an F/A-18 undergoing high angle-of-attack tests at the NASA Dryden Flight Research Center, vortices emanating from the wing/fuselage leading-edge extensions burst and immerse the vertical tail in their wake. The resulting buffeting loads on the vertical tails are a concern from a fatigue standpoint. For example, for the F/A-18 aircraft, special and costly 200-flight-hour inspections are required to check for structural damage due to buffet loads. Buffeting load alleviation through the use of active controls is a promising solution to this problem. The research objective of the current work is to apply active controls technology, using a variety of force producers, to perform buffeting load alleviation on a twin-vertical-tail wind-tunnel model.

A 1/6-size, rigid, full-span model of the F/A-18 A/B aircraft was tested in the TDT. The model, shown in figure 11 mounted on a sting in the tunnel, was tested with flexible and rigid tail surfaces. Three flexible tails were built to test different control concepts. The flexible tails were instrumented with a root strain gage aligned to measure bending moment and with two tip accelerometers. Each tail was equipped with a different concept for buffet alleviation: the first was equipped with an active rudder; the second could be equipped with either an active tip vane or an active embedded slotted cylinder; and the third was equipped with active piezoelectric actuation devices. Of the different concepts, early open-loop tests in the tunnel indicated that the rudder and the piezoelectric actuators appeared to be the most promising candidates. A photograph of the piezoelectric actuator on the flexible tail is shown in figure 12.

Two single-input/single-output control laws were implemented on the model. One control law used the rudder and the other used the piezoelectric actuator. Both control laws used a vertical tail leading-edge tip accelerometer as the sensor. The

control laws added damping to the system by providing a 90° system phase lag between the added force and the accelerometer response. The results are presented in figure 13 in terms of root bending moment versus angle-of-attack. Reductions in root bending moment as much as 60% at certain angles-of-attack are evident. Results of this investigation are to be published in [10]. The results of this wind-tunnel test illustrate that buffeting alleviation of the vertical tails can be accomplished by using the rudder or piezoelectric actuators as active controls.

TILTROTOR WING VIBRATORY LOADS REDUCTION USING ACTIVE SWASHPLATE AND FLAPERON

The fundamental vibration problem in tiltrotor aircraft is caused by blade passage in front of the wing while in high-speed airplane-mode flight. Wing circulation creates an azimuthally unsymmetric flow through the rotor system which is the primary contributor to fixed system (pylon, wing, and fuselage) vibrations. The Wing and Rotor Aeroelastic Testing System (WRATS) tiltrotor model is a semispan testbed developed from a V-22 1/5-scale aeroelastic tiltrotor model. It was designed and fabricated by Bell Helicopter Textron, Inc. (BHTI). In an effort to control vibrations in the fixed system, BHTI developed a system called the Multipoint Adaptive Vibration Suppression System (MAVSS). The objective of the current research is to evaluate the ability of the MAVSS system to control multiple modes of fixed-system vibrations on the WRATS model during tests in the TDT.

A photograph of the WRATS model mounted in the TDT is shown in the figure 14. An active control system using three high-frequency hydraulic actuators to tilt the swashplate and an active flaperon was fabricated and installed on the WRATS model. The actuators were driven by a signal produced by the MAVSS system at frequencies up to 50 Hz. The basic test procedure was to identify flight conditions of high vibration, activate MAVSS, and compare the resulting loads. The MAVSS system operates in the following manner: It obtains feedback signals from response sensors (beam, chord, and torsion strain gage bridges); quantifies model vibration levels in an objective function; identifies the system using a series of test signals; computes and then applies commands to the active swashplate/flaperon to lower the objective function. If the optimized vibration level rises above a given

threshold, the controller will automatically reactivate itself.

The bar chart shown in figure 15 contains results from the wind-tunnel test and illustrates the success of the MAVSS system in controlling vibratory loads in three wing modes simultaneously. Each set of three vertical bars grouped together indicates the three-per-rev (3P) wing beam, chord, and torsion loads at one instant of time. For each of the four airspeeds there are a set of bars shown with the MAVSS system both off and on. The plot shows a trend of increasing baseline 3P vibration level in all three wing modes with airspeed, but, more importantly, also shows significant reductions (89% to 99%) in all 3P vibratory wing loads at each airspeed. Although not shown on the figure, the swashplate and flaperon motions required to accomplish these reductions are within acceptable limits. Results of this investigation will be fully documented in [11]. This test has confirmed that an active control system is a viable candidate for alleviating multiple modes of tiltrotor vibration.

PHOTOGRAMMETRIC APPENDAGE STRUCTURAL DYNAMICS EXPERIMENT

The Photogrammetric Appendage Structural Dynamics Experiment (PASDE) was developed to demonstrate the use of photogrammetric techniques for structural dynamic response measurements of spacecraft solar arrays and similar structures. Development and demonstration of passive, on-orbit structural response measurement methods will increase the amount of spacecraft engineering data available. The availability of low-cost, on-orbit engineering data for the International Space Station is essential for mathematical model and design load verification and subsequent determination of proper operational procedures and constraints.

A photogrammetric structural dynamic response measurement instrument was designed, fabricated, assembled, and tested to meet a flight experiment opportunity on a NASA Shuttle/Mir mission (STS-74) in November 1995. The instrument consisted of six video cameras with 50mm lens and motorized irises, six video tape recorders, video time inserters, and interface electronics. The instrument was packaged in three standard Shuttle canisters. A mission plan was developed to obtain video image data during STS-74 mission events considered likely to result in structural response motion of the

Mir Kvant-II module lower solar array as shown in figure 16.

The PASDE mission was implemented from a Control Center at the Goddard Space Flight Center during the mission. Video data was collected on the PASDE video recorders during the following events: docking of the Shuttle with Mir, three sets of specific Shuttle jet firing sequences designed to excite structural motion of the combined Shuttle/Mir spacecraft, transitions of the combined spacecraft from night-to-day and day-to-night, and sun tracking movements of the solar array. The video data was retrieved from the instrument following the mission, and digitized into standard computer image format. From the digitized data, displacement time histories at points in the video images were computed. The time history data was then triangulated using the known geometry of the instruments in the Shuttle payload bay and the coordinate systems of the Shuttle and Mir to obtain high resolution three-axis motions of multiple points on the solar array. A time history of the normal displacement at the point indicated by the white circle in figure 16 is shown in the graph. A description of the experiment is presented in [12].

The PASDE experiment demonstrated the use of passive photogrammetric techniques to make high resolution structural response measurements of solar arrays and other spacecraft appendages on-orbit. The International Space Station has adopted this technique for on-orbit measurement of solar array response.

INTERFACE TECHNOLOGY

Detailed analysis of complex aircraft structures can severely tax today's computing environment. Therefore, it is highly desirable to use detailed modeling only when necessary. Embedding local refinement in a single model of the entire structure may lead to highly complex modeling due to the use of transition modeling between highly refined regions and regions with less refinement. Additionally, transition modeling typically introduces distorted elements into the finite element model which may adversely affect the accuracy of the solution.

Interface technology was developed [13] that allows the independent modeling of different substructures or components without the concern for one-to-one nodal coincidence between the

finite element models. The interface element acts as a "glue" between independent finite element models with different mesh densities and nodal layouts. Interface technology provides a local/global model which is fully coupled, has displacement compatibility, and captures changes in load and load path. Interface technology provides the analyst with increased modeling flexibility. Since the grid points along the common substructure boundaries need not coincide, the need for potentially complex transition modeling is eliminated. Different levels of approximations may be used in each of the substructures allowing the use of substructures only where needed. Examples of how this technology can be used are presented in figure 17. An example of interface technology applied to a built up fuselage panel is presented in figure 18. This technology provides a means of rapidly assembling diverse structural models subject to mechanical, thermal or dynamic loads. These models can come from different sources or from previous designs where similar components were used. The engineer working on preliminary vehicle design could create structural models of unparalleled accuracy by combining components from a "library" of models. Structural modeling assembly and design could become a "plug and play" operation.

CRASHWORTHINESS

The objectives of crashworthiness research are to develop a fundamental understanding of the response of composite structures to impact loads, and to apply this information for improved crashworthiness designs [14]. The crashworthiness program has four main elements: full-scale crash testing, crash analysis, scale model testing, and the development of innovative concepts for improved crashworthiness. A recent accomplishment in this program was the full-scale crash test of an all-composite Lear Fan 2100 aircraft. NASA acquired two prototype aircraft after the company ended production. The aircraft was never put into production.

The Lear Fan aircraft is fabricated of graphite epoxy composite material with construction that consists of semi-circular frames which are bonded and riveted to the skin. The subfloor of the aircraft contains four longitudinal aluminum beams which were used for grounding and lightning protection. The presence of the aluminum subfloor beams can cause the impact response of this composite aircraft to be

similar to those of previously tested metallic general aviation aircraft. Therefore, the first Lear Fan aircraft was tested with the aluminum beams in place. For the second Lear Fan aircraft, the aluminum subfloors will be removed and an energy absorbing composite subfloor will be installed. Both aircraft are to be tested under identical impact conditions of 82 ft/sec horizontal velocity, 31 ft/sec vertical velocity, and a flat impact attitude. On board the aircraft were side-by-side seat tests with one anthropomorphic dummy seated in a standard GA aircraft seat (pilot), and a second dummy seated in an energy absorbing seat (co-pilot).

A photograph of the aircraft undergoing flight testing is shown in figure 19. A post-test photograph of the aircraft after crash testing is also shown in the figure. Post-test damage assessment indicated a large fracture in the top of the fuselage, several smaller fractures emanating from the doors and windows, and all the composite frames were fractured close to the impact point. No damage was observed in any of the aluminum floor beams. Measured acceleration levels at the floor location were in the range of 160-200 g's. As shown in figure 19, the energy absorbing seats offered more protection to the occupant than did the standard seat. For example, the co-pilot dummy only slightly exceeded the FAR 23 requirement of no more than 1500 lb load in the lumbar region, whereas the pilot dummy seated in a standard seat exceeded the level by a factor of two. A comprehensive development program is being conducted to design a composite energy absorbing floor beam for retrofit on the second Lear Fan aircraft. Lightweight, cost-effective composite floor beam concepts are being developed to improve the energy absorbing capability of the airframe. Static and dynamic tests are being conducted on these structural concepts to determine their response characteristics when subjected to crash loads and to evaluate their energy absorbing capability.

Several composite fuselage subfloor-beam configurations have been evaluated for their static and dynamic response characteristics, their energy absorption capability, their ability to control transmitted loads, and their structural integrity after crushing. A foam-filled composite floor-beam concept has been identified that has enough energy-absorption capability to limit to an acceptable level the high-acceleration crash loads that are transmitted to a passenger seat during a crash event. Test results shown in figure 20

indicate that a relatively simple flat-sided box-beam configuration with a foam core that is integrated with an aircraft seat rail can satisfy the energy absorption, load transmission level, and structural integrity goals for crashworthiness. A desired, relatively constant, collapse load, designated as the Sustained Crush Load (SCL), of 240 lbf/in. was achieved with the concept as shown in the figure. A SCL value of 200 - 300 lbf/in. is generally required for crashworthiness. The load attenuation characteristics of the test specimen are excellent as shown in figure 20. Approximately 230 g's of acceleration force was imposed on the test specimen and a response of approximately 25 g's was recorded.

The results of the tests with the foam-filled composite floor-beam concept indicate that it is possible to design energy-absorbing crashworthy composite structures. The results of these tests will help designers of future aircraft fuselage structures develop designs with improved energy-absorbing subfloors.

COMPOSITE STRUCTURES

For three decades, NASA has worked in close partnership with the U.S. aircraft industry to develop the materials, the structures, and the essential science that provides the means to fully exploit the use of composites in aerospace vehicles. Throughout this period, NASA has supported the development of materials synthesis, structural analysis methods, fracture mechanics, and test procedures. Building upon this essential science foundation, the aircraft industry has systematically explored the application of composite aircraft structures. NASA and industry began in the 70's to develop lightly loaded aircraft components such as spoilers for the Boeing 737 and upper aft rudder for the Douglas DC-10. A significant number of these structures were built, ground tested, and subjected to long-term flight tests. This work established industry confidence in the performance and environmental durability of composites for aircraft use. In the decade of the 80's, NASA and industry focused their development efforts on medium-loaded primary structures that included the horizontal stabilizer for a Boeing 737 and the vertical stabilizer for the Douglas DC-10. These primary components received FAA certification and are still in flight service.

NASA studies in the mid 80's established that the full potential of composites in aircraft could only be

achieved with the development of composite wing and fuselage structure. The major barriers were recognized to be damage tolerance and cost. In 1989 NASA launched its Advanced Composites Technology (ACT) Program aimed specifically at developing cost-effective composite primary structures for commercial transports. While this work has not reached the technology readiness level required for industry to produce a new aircraft with a composite wing or fuselage, significant progress has been made. This progress includes: (1) a basic understanding of compression strength after impact damage, (2) new materials and approaches for increasing compression strength after impact damage, (3) materials data base, (4) tests methods and analysis, (5) repair approaches, and (6) exploring new fabrication methods to reduce costs.

One of the primary goals of the ACT program is to develop the enabling technology that will allow composite materials to be used in the primary wing and fuselage structures of the next generation of advanced subsonic transport aircraft. Composite structures offers the greatest potential for reducing the direct operating cost (>10%), reducing weight (up to 40%), and the elimination of corrosion and fatigue issues. The following sections will describe research activities that are being pursued in both wing and fuselage technology.

Wing Stub Box

To evaluate the potential of a stitched graphite-epoxy material for use on commercial transport aircraft wings, a section of a wing box was designed and fabricated by the McDonnell Douglas Aerospace Company under the NASA ACT program. The wing stub box represents the inboard portion of a high-aspect-ratio wing box for a civil transport aircraft. The wing box was fabricated using an innovative manufacturing process that has potential for reducing manufacturing cost and producing damage tolerant composite primary aircraft structure. The objectives of the tests were to evaluate the behavior of a wing box structure and to verify analysis methods for predicting the structural response of the wing box [15 and 16]. The wing box was designed to simulate a section of a commercial transport wing and was subjected to bending loads.

As shown in figure 21 the wing stub box test specimen consists of a metallic load transition

structure at the wing-root, a composite wing stub box, and a metallic extension structure at the wing-tip. The load transition structure and the wing-tip extension structure are metallic end fixtures required for appropriate load introduction into the composite wing stub box during the test.

Layout of the composite stub box is shown in figure 22. The stub box consists of ribs, spars, and upper and lower cover panels (each of which has stringers and intercostals stitched to the skin). The skin of the upper and lower cover panels range in thickness from about 0.29 to 0.90 inches. The upper cover panel has 10 stringers along the length of the wing box and the lower cover panel has 11 stringers. The upper cover panel has an access door cutout. At the stringer runout locations, the stringer is terminated and the tapered stringer web provides a mechanism for smoothly transferring the load from the stringer to the skin. At the runout, fasteners were installed to prevent skin stiffener debonding at these locations. The ribs and spars were stiffened with blade stiffeners to prevent buckling. The ribs were connected to the cover panels at the intercostals.

A series of structural tests were conducted by loading the wing in bending with no damage, with detectable damage, with nondetectable damage, and with a repair. Damage was inflicted to the upper cover panel by using a dropped-weight impactor. Strains at 254 locations and displacements at 15 locations on the structure were recorded during each test. A photograph of the wing stub box prior to testing is shown in figure 23.

No failures and no damage growth occurred in preliminary tests of the undamaged structure with the applied load up to Design Limit Load (DLL). The structure satisfied the requirement of supporting DLL with detectable damage caused by dropped-weight impact condition imposed on the wing box. The damaged region was repaired with a simple aluminum bolt-on patch by American Airlines maintenance personnel.

In the final test the structure supported 140% of DLL prior to failure through a stiffener runout region with nondetectable impact damage. Two independent failures occurred in the stub box. The first failure occurred in an unsupported region at the runout of a stringer where it terminates at a rib (in the same bay as the access panel cutout). The stringer had extensive damage including delaminations

between the skin and flange, broken stitches, bolts pulled through the flange, and cracking of the blade. This failure involved large out-of-plane deformations in the upper cover skin bay outboard of the access door. The second failure was catastrophic and initiated at a nondetectable impact damage sight. The failure occurred across the entire width of the upper cover panel and into both spars. The maximum load carried by the structure was 154 kips (93% of design ultimate load). A view of the failure is shown in figure 24.

The other objective of the test was to verify analytical methods for predicting the structural response of the wing box. An initial finite element model [17] accurately predicted the global behavior of the stub box but did not accurately predict the behavior at the center portion of the upper cover panel outboard of the access door or at the splice joint between the composite stub box and the metallic extension box. A refined model was created to improve the accuracy of the analytical predictions. A comparison of strain response between the original and refined analyses and experiment is shown in figure 25.

The tests verified the ability of the wing box structure to satisfy most of the design requirements. The global behavior of the structure is in good agreement with the analytical predictions and the displacements and strains predicted by a geometrically nonlinear analysis using a refined finite element model compare very favorably with experiment.

Fuselage Structures

As part of the ACT program, the Boeing Commercial Aircraft Group has been working to develop cost effective and structurally efficient composite fuselage structure. The focus of this work has been on the fuselage section just aft of the main landing gear wheel well of a modern wide body transport as shown in figure 26. This fuselage section is 33 feet long and 20 feet in diameter and contains crown, side, and keel quadrant sections as shown in the figure. Sandwich structure is being considered in the design of side and keel quadrant sections because it has the potential for high structural efficiency and low cost manufacturing.

The application of sandwich structure has been restricted in the past due to undesirable moisture absorption and retention, and due to an insufficient

understanding of low-speed impact damage mechanisms and the effect of such damage, as well as penetration damage, on the structural performance of sandwich structures.

Understanding these issues are important if composite sandwich concepts are to be accepted for primary structures. A joint NASA/Boeing study of the technology issues associated with the use of composite face sheet sandwich construction in the side and keel panels is being conducted as part of the ACT program [18 and 19].

Keel Panel

A composite sandwich fuselage keel test panel was fabricated by the Boeing Commercial Airplane Group, and is representative of a highly loaded fuselage keel structure (figure 27). The test panel was machined from a larger demonstration panel that was fabricated to gain experience with tow placed composite structures with dropped plies. The dropped plies result from the reduction in compression loads as the structure moves aft in the keel section. The purpose of these studies is to understand the load distribution in thick-face-sheet composite honeycomb-sandwich structures with and without impact damage, and to understand the load distribution and panel failure mechanisms in the presence of both impact damage and discrete-source damage. Compression tests of the panel with three different conditions were conducted: undamaged; barely visible impact damage (BVID) in two locations; and with BVID in two locations and a notch through both face sheets. The impact-energy level necessary to inflict BVID on the panel was determined from an impact-damage screening study conducted on another panel of the same design. BVID was assumed to have occurred when the residual dent depth on the facesheet at the impact location was equal to or greater than .05 in. or the impact energy was greater than 100 ft-lbs. Finite element analyses of the undamaged panel and the notched panel were also performed.

The tests of the impact damaged and notched panel identified the notch as being the most critical of the three damage sites. Analytical results compared well with the experimental results. The notched panel failed at 202 kips, which is the design ultimate load for the panel. The failure mode was compression failure of the face sheets at the notch location. A photograph of the failed panel is shown in figure 28. Since the panel supported

design ultimate load with BVID, the design is damage tolerant for nonvisible impact damage.

An important finding from the impact-damage screening study [18] was that significant internal damage occurred at relatively low impact-energy levels and that the corresponding surface damage at the impact sites as measured by the residual dent depth were very small, making it nonvisible to a ground-crew inspection. This internal damage at the impact locations can significantly reduce the residual strength of the panel. These results suggest that the present approach of using residual dent depth as a means of assessing the effect of BVID on the strength degradation of a composite honeycomb-sandwich structure needs to be re-evaluated.

To identify a more suitable criterion for assessing the effects of BVID on the strength degradation of thick-face-sheet composite honeycomb-sandwich structure, compression-after-impact residual-strength studies were performed on specimens that have been impacted with a wide range of damage-inducing impact-energy levels [19].

For this study, 5 inch wide by 10 inch long specimens were machined from the original keel demonstration panel. These specimens were tested in compression in both the undamaged and damaged conditions. A typical test set up in a 300 kip testing machine is shown in figure 29. Impact damage was generated using a dropped weight impact apparatus. Impact energies ranged from 40 ft-lbs to 100 ft-lbs. The damage area was measured from ultrasonic C-scan images of the damage site. Impact screening tests that were performed earlier indicated that significant internal damage can occur for impact energies significantly lower than 100 ft-lbs even when the residual depth dent is much smaller than .05 in.

Results for seven specimens are presented in figure 30. As shown in the figure global stiffness (except for specimen 6) of the specimens is not affected by the impact damage. However, as shown in figure 31, failure loads as high as 40% lower than the undamaged specimen were experienced by panels with impact damage as low as 40 ft-lbs and with residual dent depth less than .01 in. Appreciable reductions in compression strength occurred for all specimens even for conditions where the impact damage would be considered non-visible. A typical failure is shown in figure 32.

As shown in the figure, a compression failure occurred in the facesheet that was impact damaged. Following this failure, the sandwich specimen experienced significant bending and the remaining facesheet failed in bending. Results from ultrasonic C-scan inspections of the impacted specimens indicated that large areas of internal damage were caused by the impact. It appears as a result of these studies that further investigation is required to establish a criteria for the affect of impact damage on composite sandwich structures.

Crown Panel

Another study being performed in support of the ACT program is shown in figure 33. Shown in figure 33 are the results of an all composite crown panel tested in the pressure box test machine. The objective of this test was to evaluate the performance of a stiffened composite fuselage crown panel fabricated using cost-effective manufacturing techniques and subjected to internal pressure and axial loads.

A fuselage crown test panel shown in the figure was fabricated by the Boeing Commercial Airplane Group, and is representative of a fuselage crown structure designed for internal pressure and high axial tension loads. The skin of the panel was tow-placed from a graphite-epoxy material system. The frames were fabricated using a braided fiber preform cured by the resin transfer molding process and secondarily bonded to the skin. The stringers were fabricated from graphite-epoxy tape and cocurred with the skin. There are no shear clips that connect the stringers to the frames at the frame-stringer intersections or "mouse-hole" regions. The fuselage crown panel was subjected to internal pressure and axial loads in the pressure-box test machine. A finite element analysis was conducted and the results of the analysis were correlated with test results.

The panel was loaded to 4,000 lb/in. of axial load and 11 psi of internal pressure prior to failure. The effect of combined internal pressure and axial load on the local bending gradients was studied. The effect of load eccentricities on panel response was studied analytically. The effect of combined internal pressure and axial load on local bending gradients was determined. The failed panel is shown in the figure.

The composite fuselage crown panel structural response was not influenced by axial loading eccentricities. Combinations of axial load and pressure influenced the bending stresses at the frame-stringer intersection or mouse hole region. The test results verified the structural integrity of this advanced design concept.

SUMMARY

This paper has presented the results of some recently completed research programs in structures at the NASA Langley Research Center. The results that have been presented indicate the wide range of research being conducted. NASA will continue to conduct research in this area in an effort to fully understand and predict structural response of aerospace vehicles so that future designs can fully exploit these technology advances.

ACKNOWLEDGMENT

The author wishes to acknowledge the work of the members of the Structures Division at NASA Langley Research Center whose research is being overviewed in this paper.

REFERENCES

1. Weisshaar, T. A.: Aeroservoelastic Control Concepts with Active Materials. ASME International Mechanical Engineering Congress Exposition, Special Symposium on Aeroelasticity and Fluid/Structure Interaction Problems. Proceedings of the 1994 ASME Winter Meeting, November 1994.
2. Heeg, J.: Analytical and Experimental Investigation of Flutter Suppression by Piezoelectric Actuation. NASA TP-3241, March 1993.
3. Crawley, Edward F.; and Anderson, Eric H.: Detailed Models of Piezoceramic Actuation of Beams. *Journal of Intelligent Material Systems and Structures*, Vol. 1, pp. 4-25, January 1990.
4. Heeg, J.; McGowan, A-M. R.; Crawley, E. F.; and Lin, C. Y.: The Piezoelectric Aeroelastic Response Tailoring Investigation: Analysis and Open-Loop Testing. Proceedings of the CEAS International Forum on Aeroelasticity and Structural Dynamics, Manchester, UK, June 1995.
5. Lin, C. Y.; Crawley, E. F.; and Heeg, J.: Open-Loop and Preliminary Closed-Loop Results of a Strain Actuated Active Aeroelastic Wing. 36th AIAA/ASME/ASCE/AHS/ASC Structures, Structural Dynamics, and Materials Conference, New Orleans, LA. AIAA Paper No. 95-1386, April 10-13, 1995.
6. McGowan, Anna-Maria Rivas; Heeg, Jennifer; and Lake, Renee C.: Results From Wind-Tunnel Testing from the Piezoelectric Aeroelastic Response Tailoring Investigation. 37th AIAA/ASME/ASCE/AHS/ASC Structures, Structural Dynamics, and Materials Conference, Salt Lake City, Utah. AIAA Paper No. 96-1511, April 15-17, 1996.
7. Rivera, Jose A., Jr.; Dansberry, Bryan E.; Farmer, Moses G.; Eckstrom, Clinton V.; Seidel, David A.; and Bennett, Robert M.: Experimental Flutter Results With Steady and Unsteady Pressure Measurements of a Rigid Wing on a Flexible Mount System. AIAA 91-1010, April 1991.
8. Farmer, M. G.: A Two-Degrees-of-Freedom Flutter Mount System with Low Damping for Testing Rigid Wings at Different Angles of Attack. NASA TM-83302, 1982.
9. Scott, R. C.; Wieseman, C. D.; Hoadley, S. T.; and Durham, M. H.: Pressure and Loads Measurements on the Benchmark Active Controls Technology Model. AIAA 35th Aerospace Sciences Meeting and Exhibit, January 1997.
10. Moses, R. W.: Active Vertical Tail Buffeting Alleviation on a Twin-Tail Fighter Configuration in a Wind Tunnel. Proceedings of the CEAS International Forum on Aeroelasticity and Structural Dynamics, June 1997.
11. Nixon, M. W.; Kvaternik, R. G.; and Settle, T. B.: Tiltrotor Vibration Reduction Through Higher Harmonic Control. American Helicopter Society Forum 53, Virginia Beach, Virginia, April 29-May 1, 1997.

12. Gilbert, M. G.; and Welch, S. S.: STS-74/MIR Photogrammetric Appendage Structural Dynamics Experiment. 37th AIAA/ASME/ASCE/AHS/ASC Structures, Structural Dynamics, and Materials Conference, Salt Lake City, Utah. AIAA Paper No. 96-1493, April 1996.
13. Ransom, J. B.; McCleary, S. L.; and Aminpour, M. A.: A New Interface Element for Connecting Independently Modeled Substructures. AIAA Paper 93-1503, 1993.
14. Jones, L. E.; and Carden, H. D.: Composite Aircraft Crash Testing. Aerospace Engineering, December 1995.
15. Jegley, D. C.; and Bush, H. G.: Test Documentation and Results of the Structural Tests on the All-Composite McDonnell Douglas Wing Stub Box. NASA TM-110204, 1996.
16. Wang, J. T.; Jegley, D. C.; Bush, H. G.; and Hinrichs, S. C.: Correlation of Structural Analysis and Test Results for the McDonnell Douglas Stitched/RFI All-Composite Wing Stub Box. NASA TM-110267, July 1996.
17. Wang, J. T.: Global and Local Stress Analyses of McDonnell Douglas Stitched /RFI Composite Wing Stub Box. NASA TM-110171, March 1996.
18. McGowan, D. M.; and Ambur, D. R.: Compression Response of a Sandwich Fuselage Keel Panel With and Without Damage. NASA TM-110302, February 1997.
19. McGowan, D. M.; and Ambur, D. R.: Damage-Tolerance Characteristics of Composite Fuselage Structures With Thick Facesheets. NASA TM-110303, February 1997.

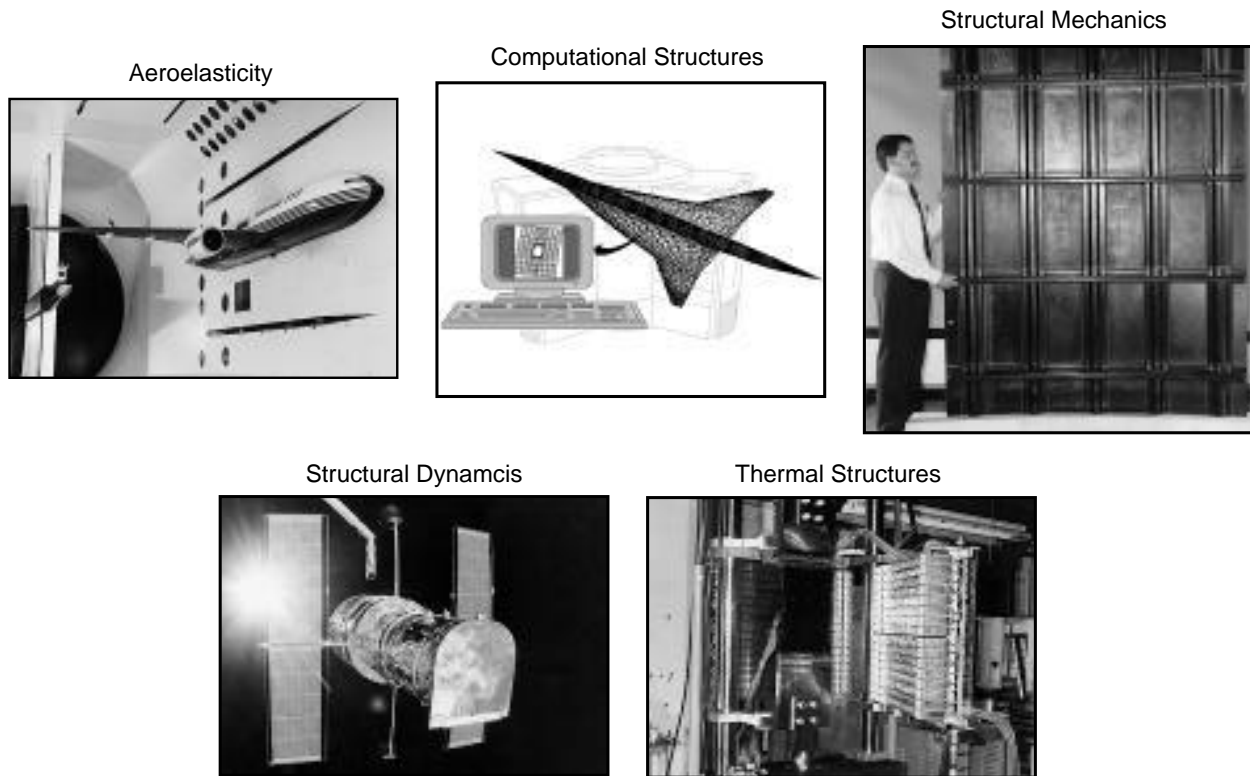


Figure 1. Structures Division research areas.

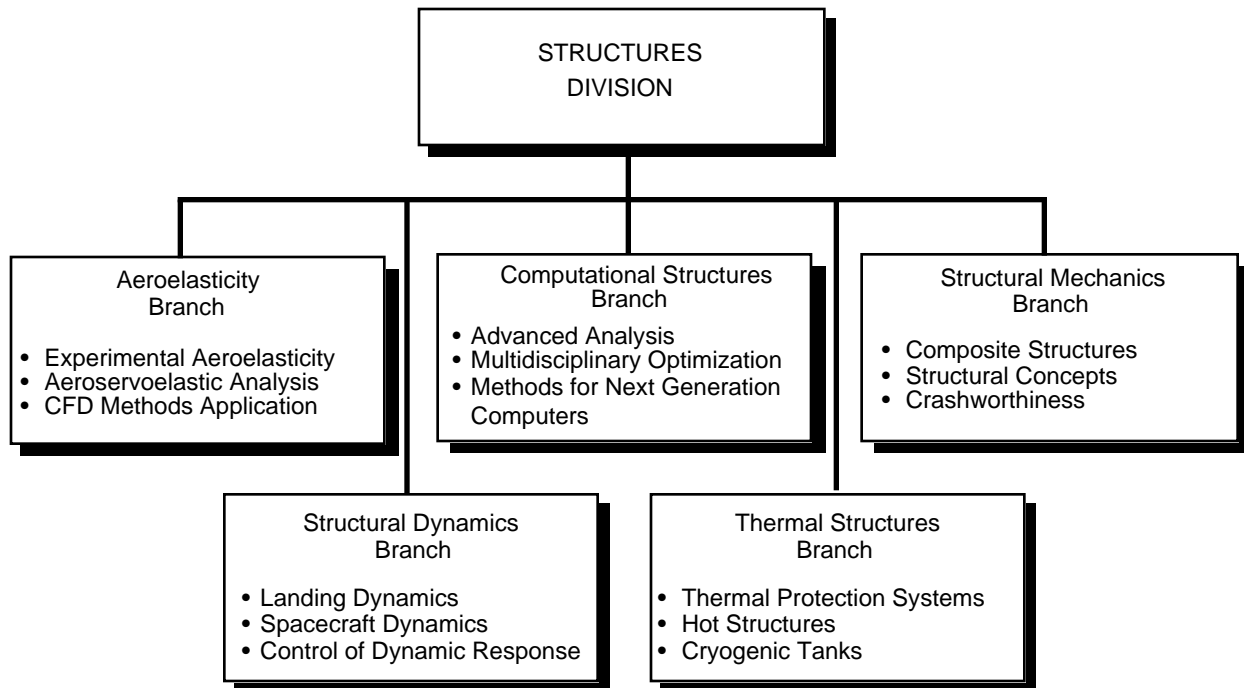


Figure 2. Structures Division research charters.

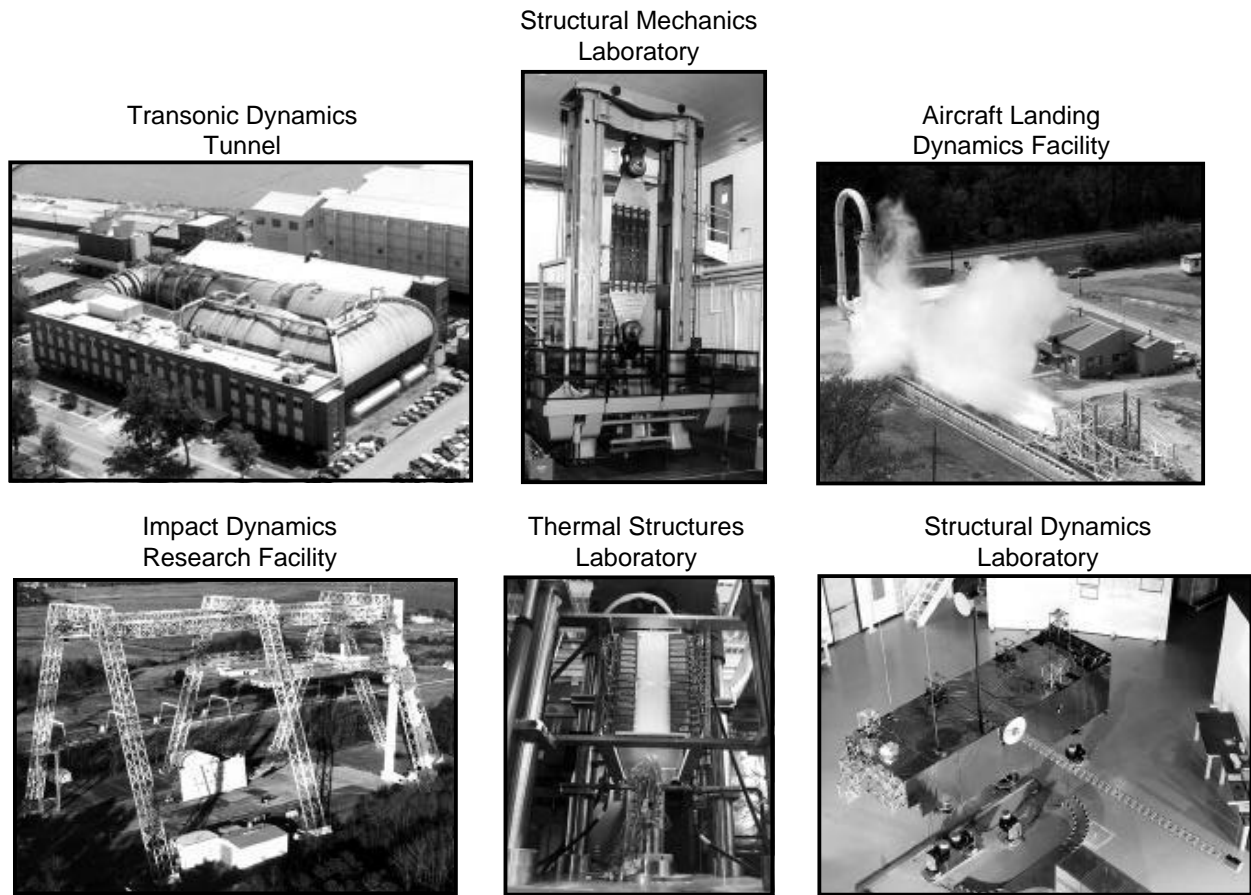


Figure 3. Structures Division research facilities.

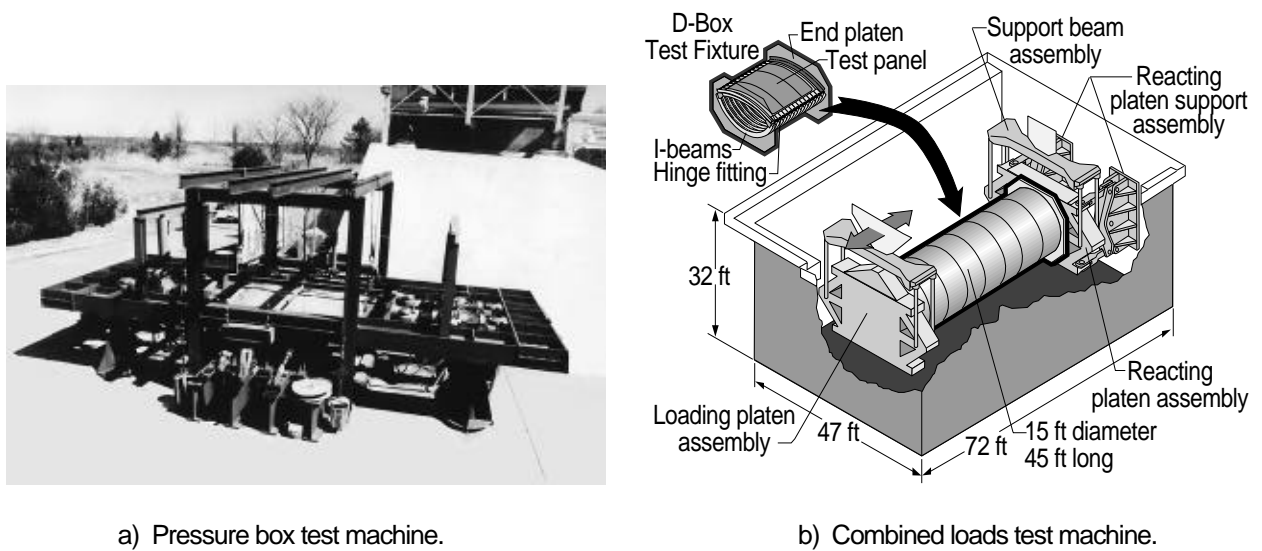


Figure 4. Combined loads testing system.

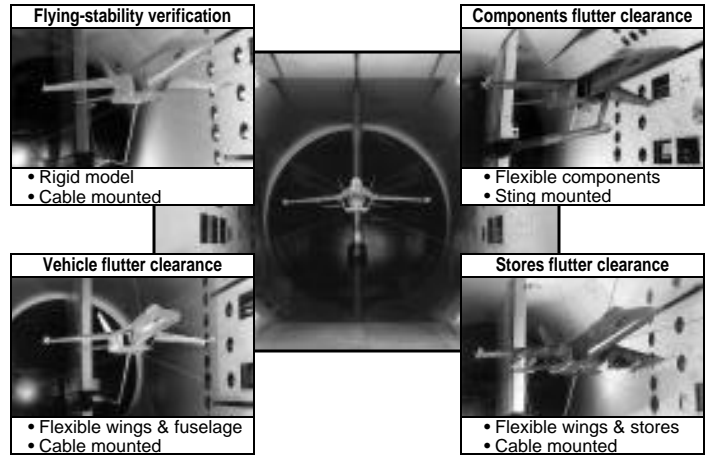
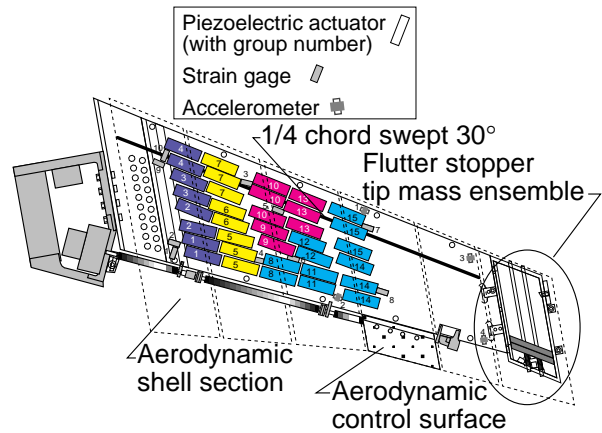


Figure 5. F/A-18 E/F flutter clearance program.

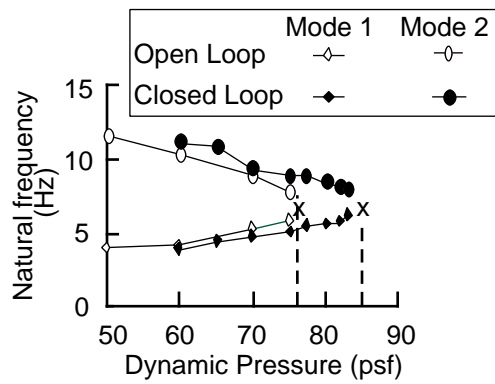


a) Model mounted in the TDT.

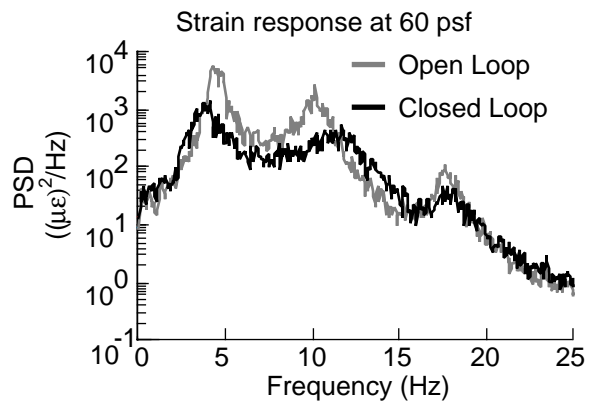


b) Sketch of major components.

Figure 6. Piezoelectric aeroelastic response tailoring investigation.



a) Flutter results.

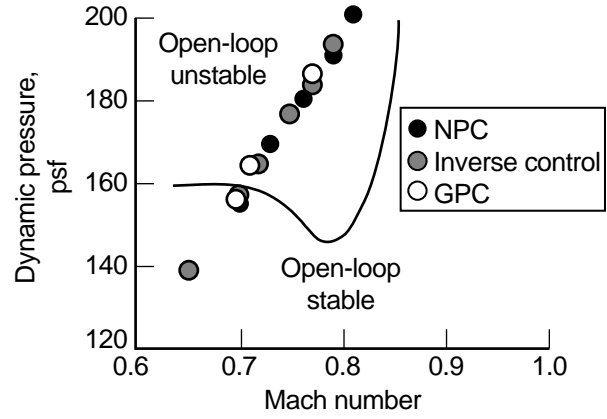


b) Subcritical response results.

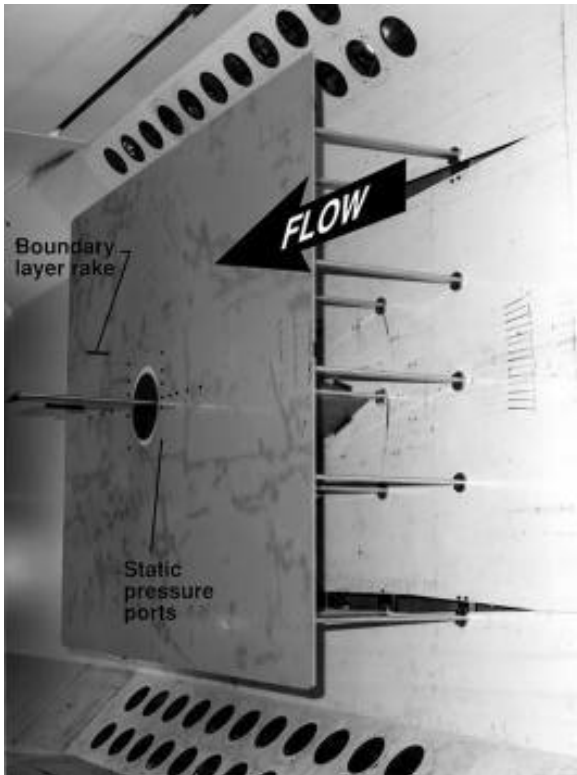
Figure 7. Experimental results.



a) Model on flexible mount.

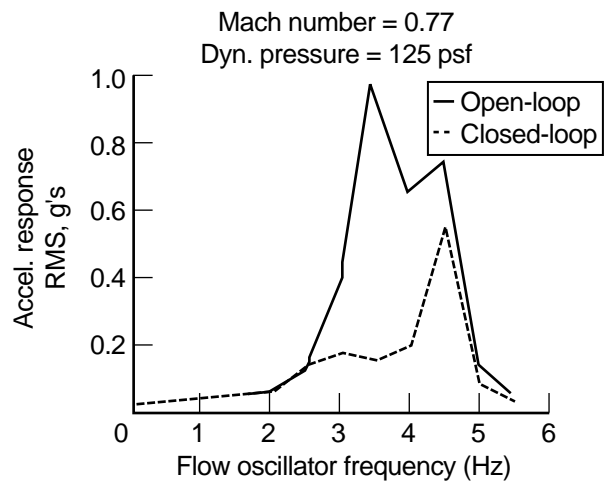


a) Flutter suppression results.



b) Model installed in the TDT.

Figure 8. Benchmark active controls model.



b) Gust load alleviation results.

Figure 9. Experimental results.



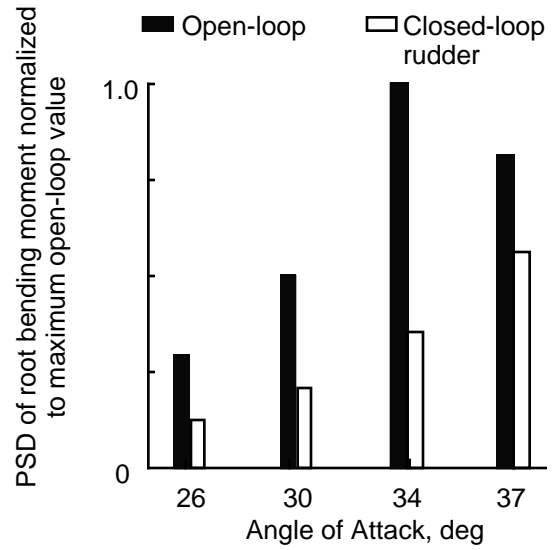
Figure 10. Leading-edge extension vortex burst on a F/A-18 at 30° angle-of-attack.



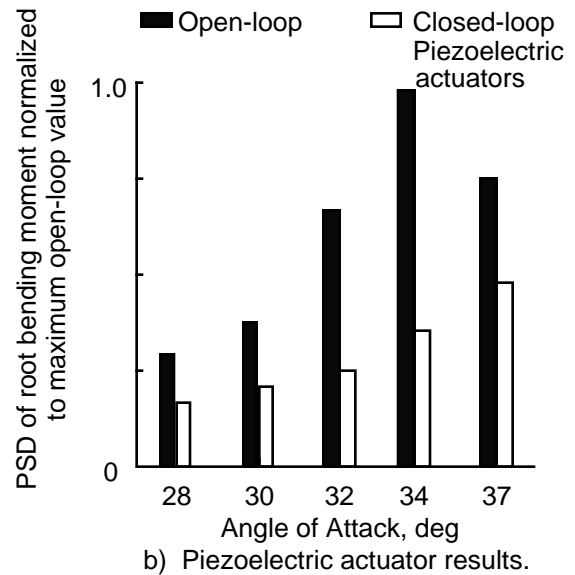
Figure 11. 1/6-scale F/A-18 model mounted in the TDT.



Figure 12. Piezoelectric actuator on flexible wing.



a) Rudder results.

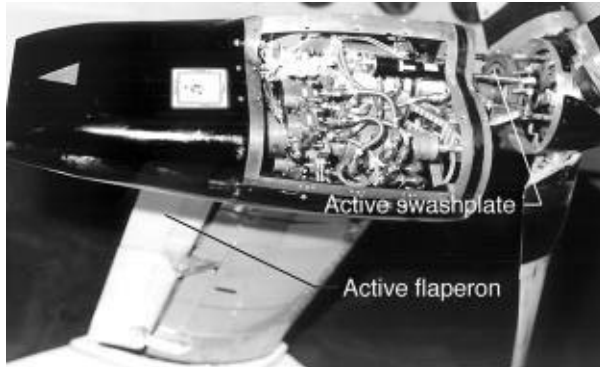


b) Piezoelectric actuator results.

Figure 13. Normalized power spectral density of root bending moment at first bending frequency for open-loop and closed-loop systems.



a) Model installed in the TDT.



b) Active control system installed on model.

Figure 14. Wing and rotor aeroelastic testing system.

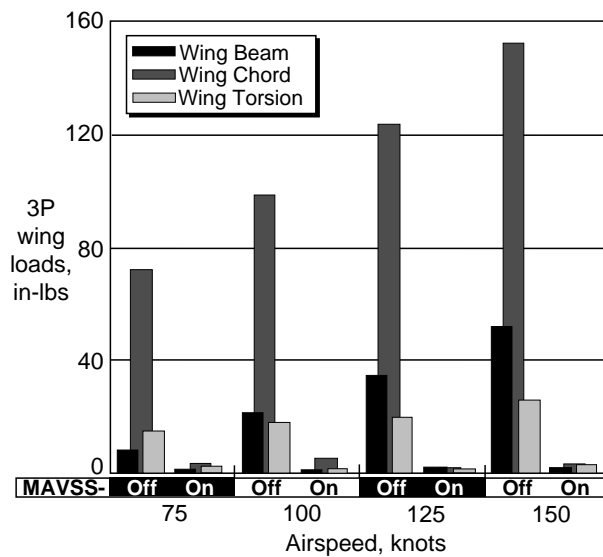
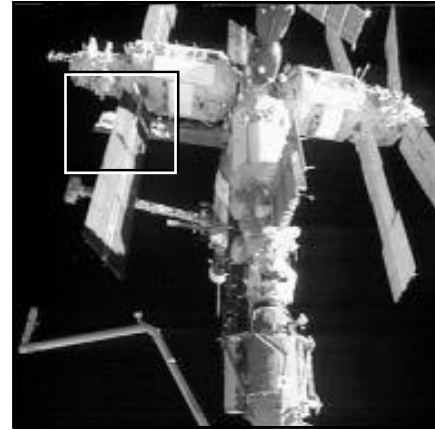
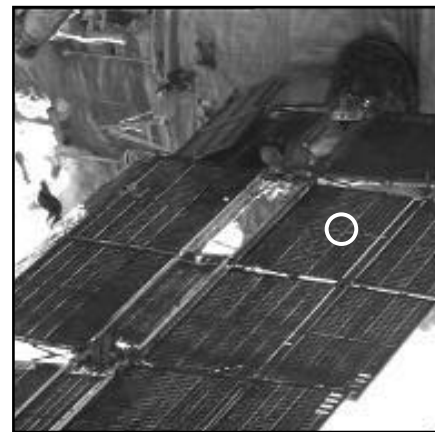


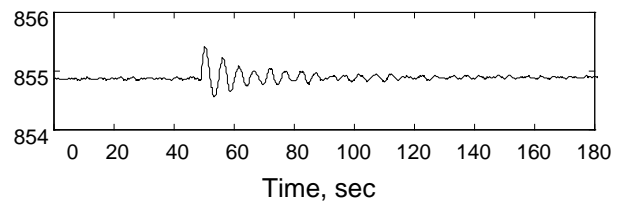
Figure 15. Effect of Multipoint Active Vibration Suppression System on loads as a function of airspeed.



a) Area of Mir imaged.



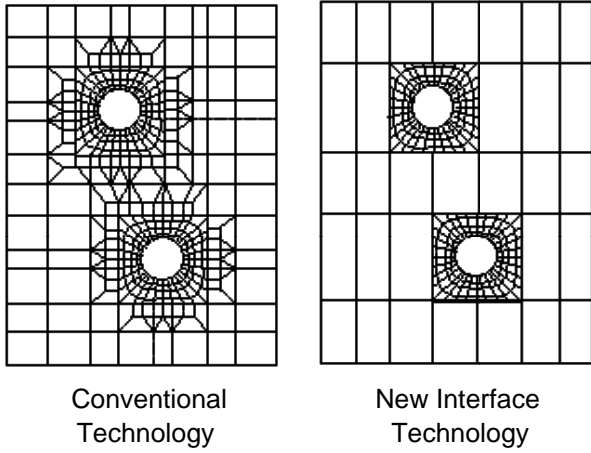
b) Data image.



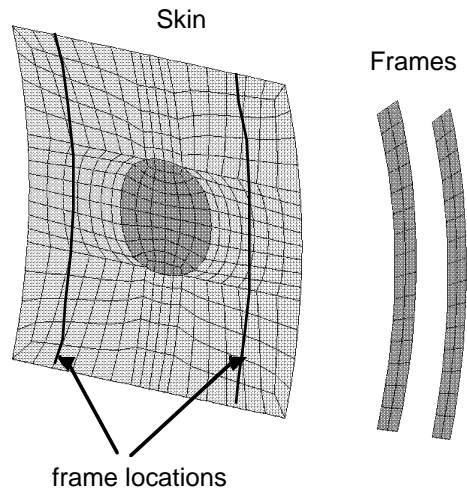
c) Displacement at \bullet due to Shuttle jet firing, in.

Figure 16. Photogrammetric Appendage Structural Dynamics Experiment.

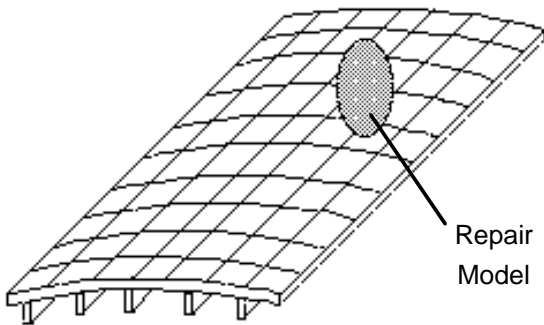
Detail Modeling



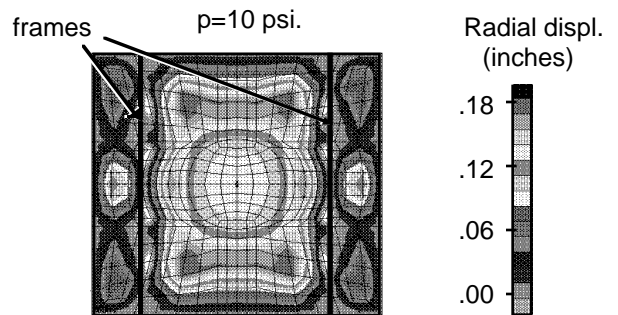
Fuselage Panel Component Models



Repair Modeling



Predicted Deformation Due to Pressurization



Assembly Modeling

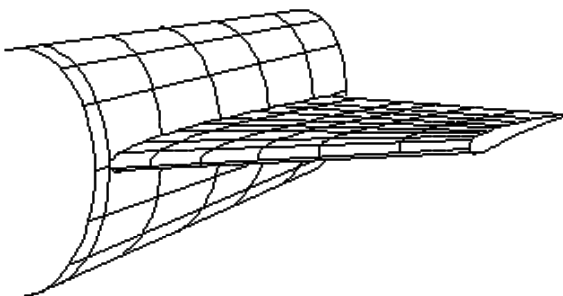


Figure 18. Demonstration of interface technology for component synthesis.

Figure 17. Interface technology applications.

Lear Fan 2100 Aircraft Pre-test



Lear Fan Aircraft Post-test



Seat Data from Lear Fan Crash Test

Pilot - Standard Non-EA Seat
Co-Pilot - JAARS EA Seat

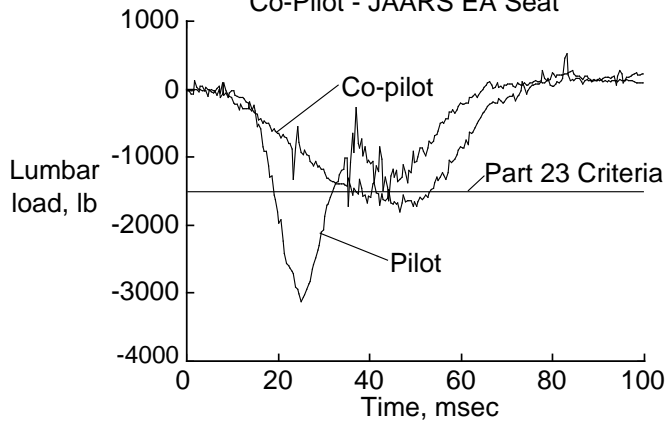


Figure 19. Crashworthiness research.

Foam filled beam with seat rail

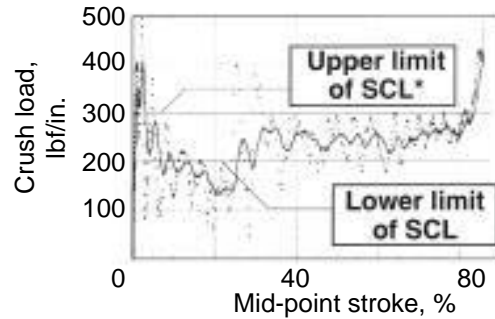
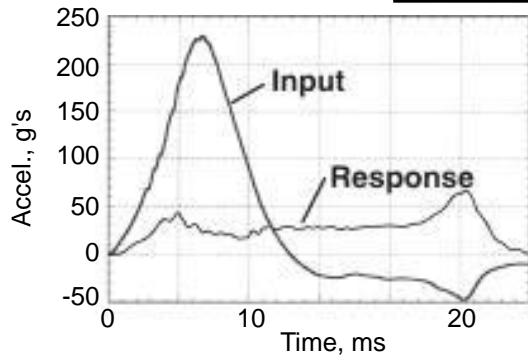
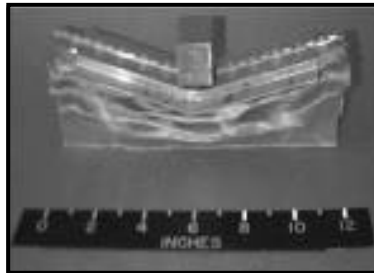


Figure 20. Composite floor beam concept.

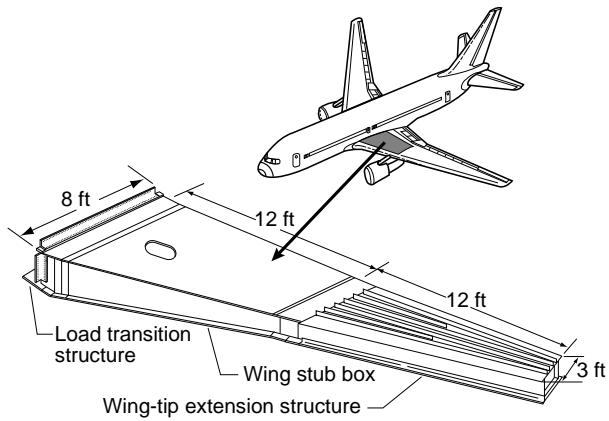
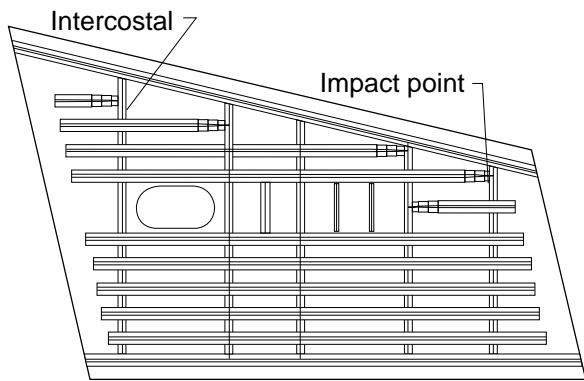
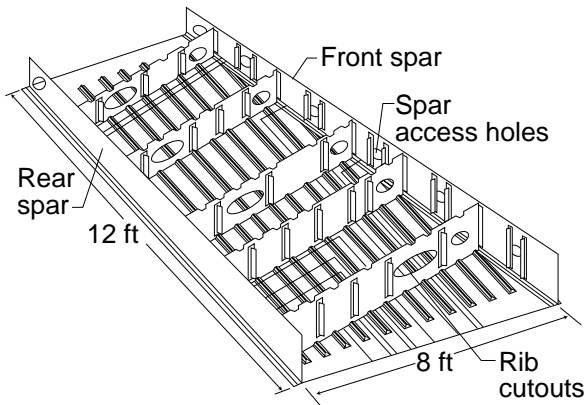


Figure 21. Wing stub box test article.



Upper cover layout



Interior of the composite stub box

Figure 22. Layout of composite stub box.

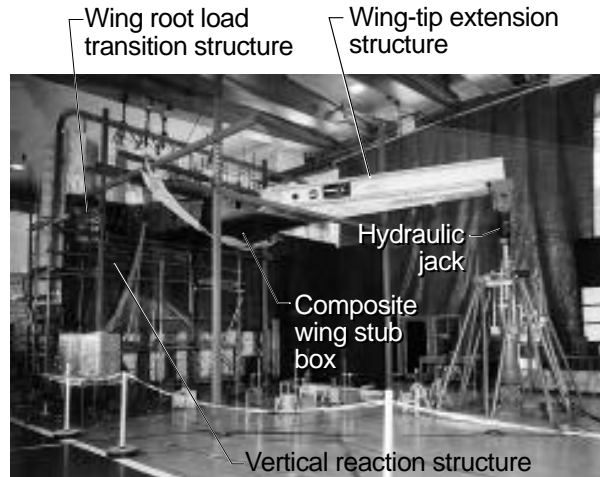


Figure 23. Wing stub box test setup.

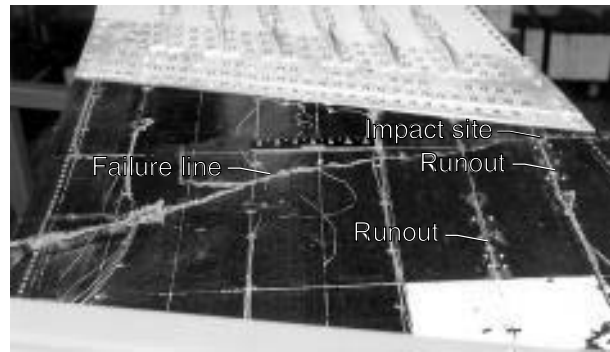
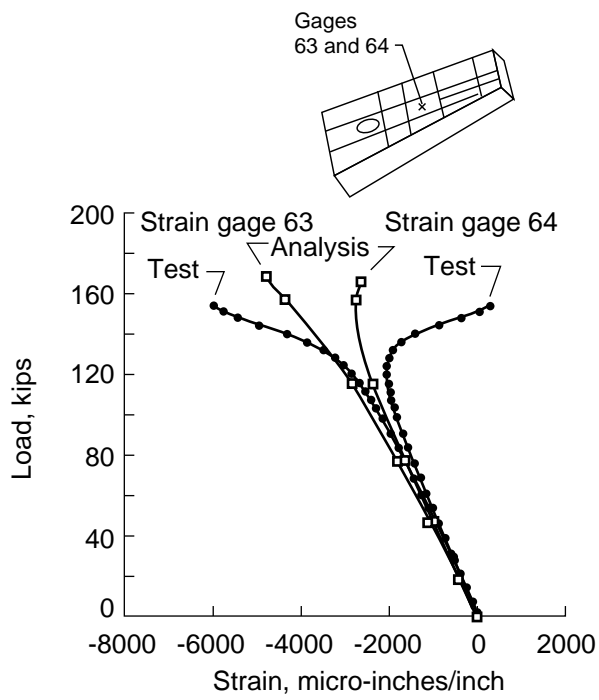
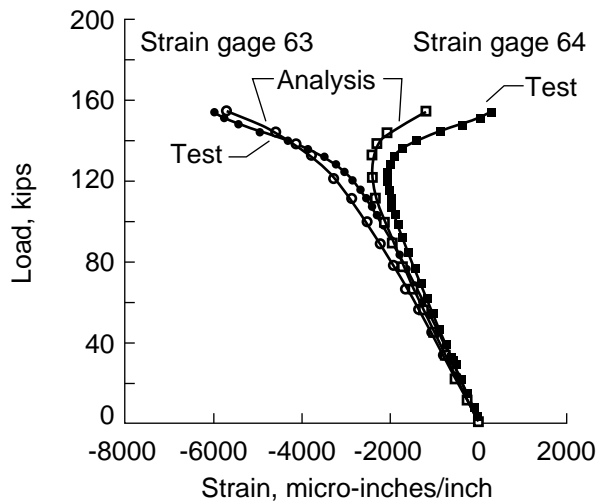


Figure 24. Upper cover of wing box after failure.



a) Initial analysis.



b) Refined analysis.

Figure 25. Comparison of strain response between analysis and experiment.

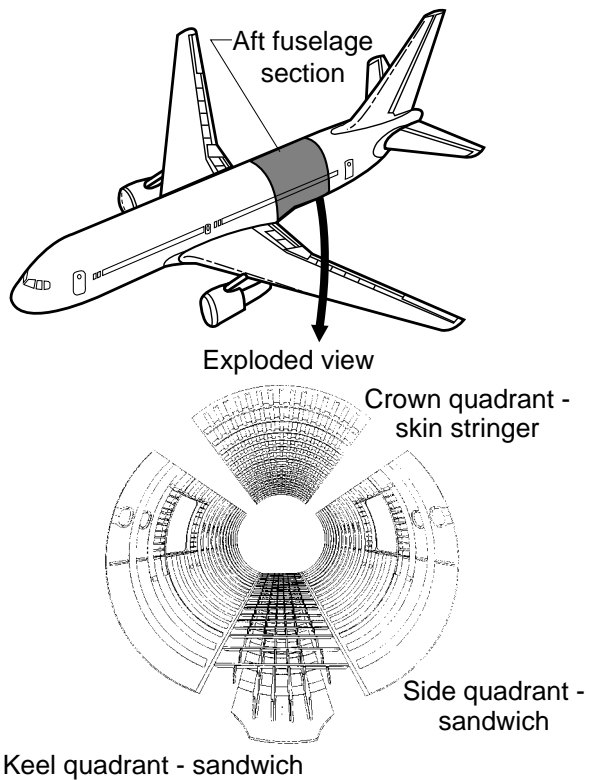


Figure 26. Generic wide-body transport aircraft fuselage structure.

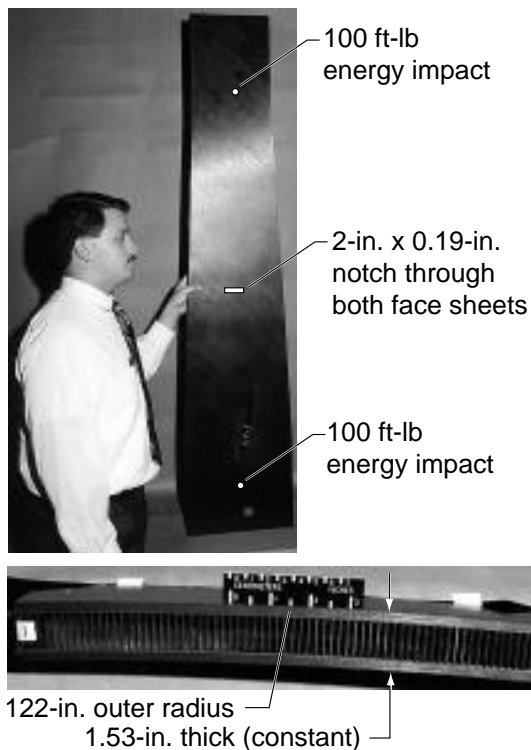


Figure 27. Forward fuselage keel panel test specimen.

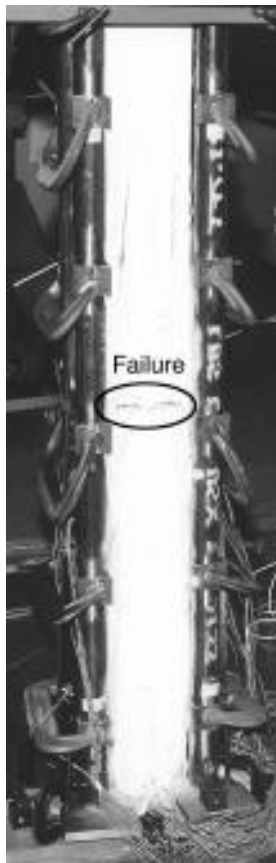


Figure 28. Failed keel panel specimen.

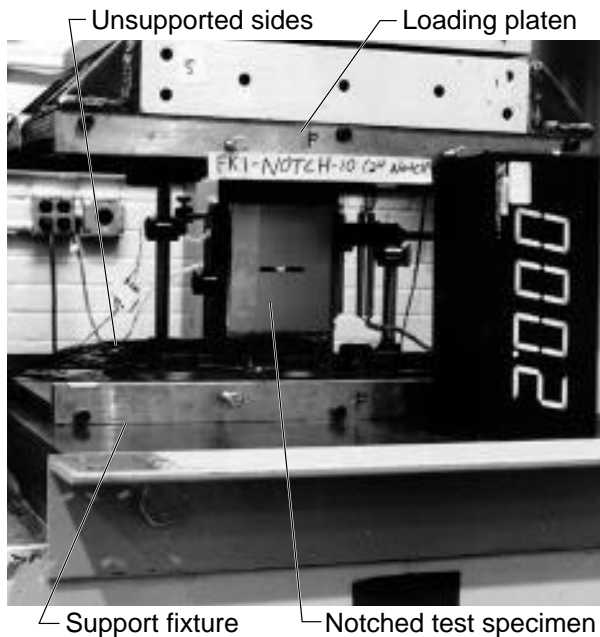


Figure 29. Typical axial compression test setup.

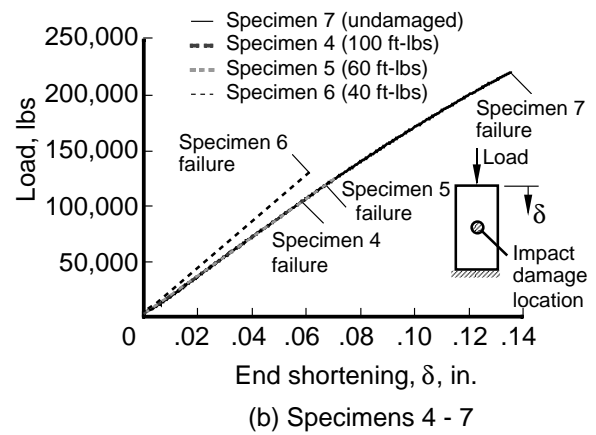
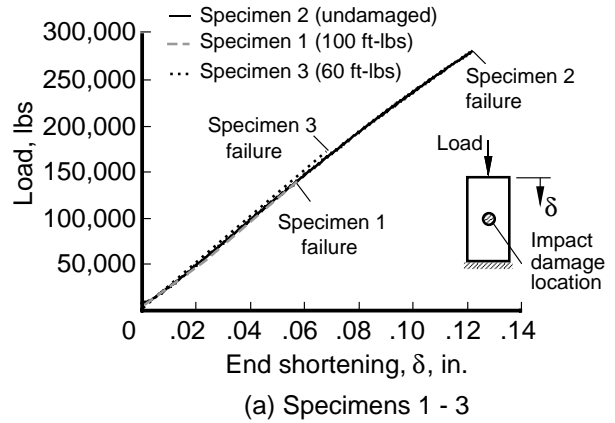


Figure 30. Experimental load-shortening results from compression after impact tests.

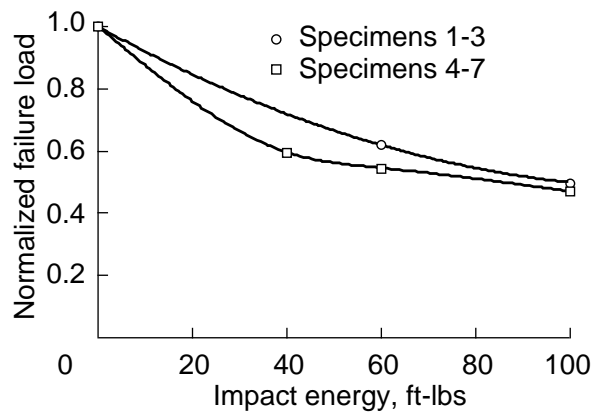


Figure 31. Normalized failure loads as a function of impact energy.

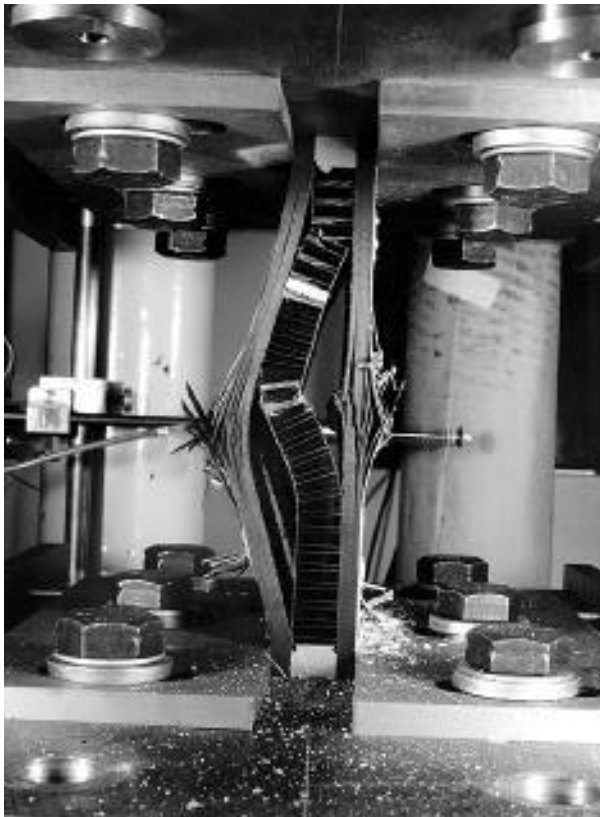


Figure 32. Typical failure mode.

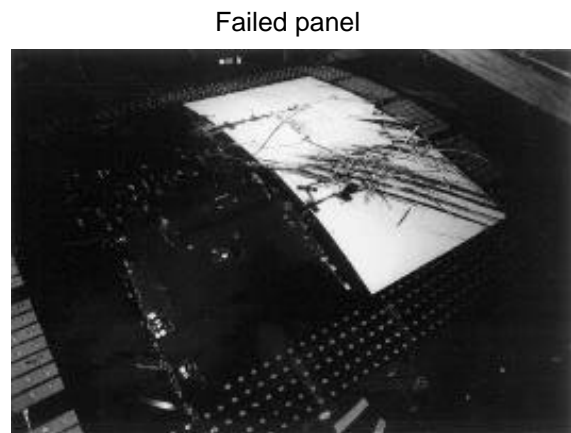
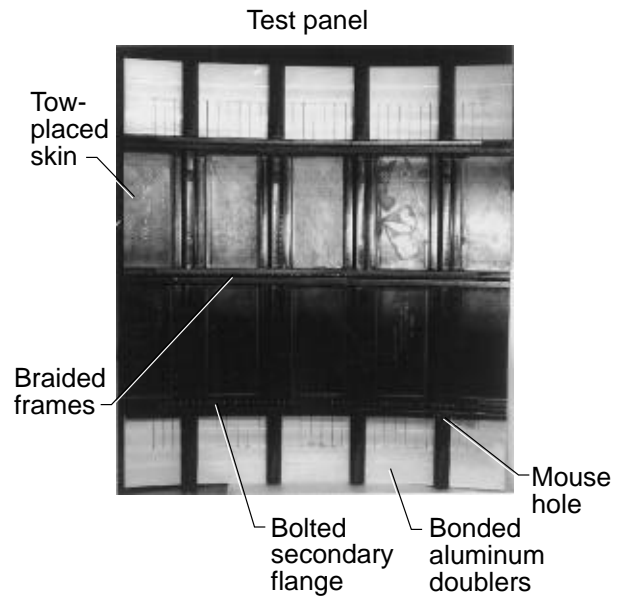


Figure 33. Composite fuselage crown panel test results.